Chapter 6

KINETIC MODELS OF COAL PYROLYSIS

In this chapter we discuss in detail relatively recent models developed in con-
nection with the experimental programs surveyed in Chapters 4 and 5. Earlier model-
ing work, now largely superseded, is altogether omitted.

The models discussed in sections 1 and 2 are phenomenological in nature. They
postulate a set of independent or coupled reactions describing product formation
in terms of various components whose exact nature remains unspecified. The postu-
lated reactions contain a number of parameters which are determined by comparison
with experimental data. In some models, the estimated parameter values fall in a
chemically meaningful range and as a result they relate to some extent to actual
chemical processes. Because of their simplicity, phenomenological models have
proved useful in combustion and gasification, where the total yield and heating
content of products are essential while the chemical structure and amount of indi-
vidual products is not required.

In the last section of the chapter, we will discuss possible approaches to
developing chemical models describing pyrolysis in terms of functional groups and
their elementary reactions. Chemical modeling has not been feasible in the past
because of the complexity of the overall process, the lack of complete grasp on
reaction mechanisms and the lack of sufficiently accurate values for rate param-
eters. Information accumulating from recent spectroscopic investigations of coal
structure and kinetic experiments with model compounds is gradually improving
this situation to the extent that chemically based models are becoming reasonable
goals in pyrolysis research. Such models would provide the theoretical framework
for further experimentation and a useful tool in process and development work,
especially in the related areas of hydropyrolysis and liquefaction in which the
chemical structure of products and intermediates is of the essence. The models
discussed in this chapter are purely kinetic. Transport processes are either
ignored altogether or are incorporated within the overall kinetics in a rudimen-
tary and empirical fashion.

6.1 INDEPENDENT FIRST ORDER REACTIONS

Although phenomenological models do not employ actual chemical structures and
elementary reactions, they do attempt to provide chemically reasonable kinetic
expressions by postulating hypothetical species participating in simple stoichi-
ometric reactions. In our discussion below, we will attempt to bring
forth the basic premises of each model as well as its utility and limitations.

6.1.1 A single first order reaction

This and the next model describe weight loss (or total volatiles) only. The simplest possible description is obviously that of a first order reaction

$$\frac{dW_v}{dt} = - kW_v \qquad\qquad\qquad (6.1)$$

$$W_v(0) = W_v^*$$

where W_v is the weight of volatile precursors in a given sample of coal of initial weight W_0, and W_v^* is the initial value of W_v, which is also the ultimate yield of volatiles, or the ultimate weight loss.

A survey of results using the simple first order kinetics of Eq.(6.1) is included in the review of Anthony and Howard (ref. 136). Three important observations made in this survey are particularly noteworthy. First, the ultimate yield W_v^* usually exceeds the proximate volatile matter (VM) of coal obtained by the well defined ASTM procedure. The ASTM procedure entails extensive secondary reactions inside and on the external surface of the coal particles. By contrast, the pyrolysis experiments of interest here relate to conditions restricting secondary reactions. This difference between the extent of secondary reactions provides an adequate explanation for the discrepancy between W_v^* and VM.

The second observation recalled from ref. 136 is that if the rate constant k is expressed in Arrhenius form,

$$k = A \exp(-E/RT) \qquad\qquad\qquad (6.2)$$

the values of A and E obtained by comparison with the experimental data exhibit large variability. In particular, values of E as low as 4 and as high as 45 kcal/gmole have been calculated while the values of A spanned several orders of magnitude. Some of this variability might be due to the difference in the type of coal but for the most it results from forcing the experimental data into a more or less arbitrary kinetic mold. As discussed in ref. 136, when a set of parallel independent first order reactions is fitted by a single first order reaction, the calculated activation energy can be smaller than each of the individual energies.

The third observation from ref. 136 is that the ultimate weight loss W_v^* often turns out to be a function of temperature, showing in a clear-cut way the deficiency of treating volatile matter as a pseudospecies. Specific results showing the dependence of W_v^* on temperature are included in Figures 4.3-4.5 of the previous chapter.

In spite of the difficulties noted above, Eq. (6.1) is often used for crude

estimates and comparisons. For example, the weight loss data from a bituminous coal and a lignite were fitted by the common parameters $W_v^*/W_o = 0.7$, $A = 6.6$ x 10^4 s^{-1}, $E = 25$ kcal/gmole (ref. 57).

6.1.2 Several first order reactions for weight loss

A conceptual improvement in the modeling of weight loss was made by Pitt (ref. 137) who treated coal as a collection of an infinite number of species decomposing by parallel and independent first order reactions. The rate constants were assumed to have common A-factor but different activation energies, varying in a range $[E_{min}, E_{max}]$ according to a probability density function, $f(E)$. Thus $f(E)dE$ is the weight fraction of volatile precursor species with rate constants having activation energies in $[E, E+dE]$. Under isothermal conditions the total weight loss is given by (6.3) where W_v^* is identified as the proximate volatile matter.

$$W_v(t) = W_v^* \int_{E_{min}}^{E_{max}} f(E) \left\{ 1-\exp\left[-t\, A\, \exp(-E/RT)\right]\right\} dE \qquad (6.3)$$

According to this equation, $W_v \rightarrow W_v^*$ as $t \rightarrow \infty$, independently of temperature. However since the pyrolysis time is limited in practice, the calculated ultimate weight loss will be temperature dependent in agreement with the experimentally observed behavior.

Expression (6.3) can be viewed as an integral equation relating the unknown function $f(E)$ to the experimentally measured function $W_v(t)$. Pitt solved this equation by an ingenious approximate technique using weight loss data from the pyrolysis of a high volatile bituminous coal at temperatures 300-650°C and times 10s-100 min. In these calculations A was given the value 10^{15} s^{-1}

Because of experimental limitations the weight loss at very short and very long times could not be measured accurately, whence the dotted sections of the curve represent an extrapolation. The weight loss calculated with the curve $f(E)$ of Fig. 6.1 was in good agreement with the experimental weight loss.

It is informative to seek possible chemical interpretation of Pitt's model. As discussed in the previous chapter, tar constitutes 75% or more of weight loss for high volatile bituminous coals, therefore, the sharp peak in Figure 6.1, at about 50 to 55 kcal, would correspond to the tar species. This behavior would be consistent with the hypothesis that the main tar forming reaction involves the dissociation of the ethylene bridge (reaction D5 in chapter 3) whose activation energy would be in the range 48-57 kcal depending on the size and the substituents of the aromatic nucleus. It must be emphasized, however, that it has not as yet been established that the dissociation of the ethylene bridge constitutes the main elementary reaction in tar production. Similar
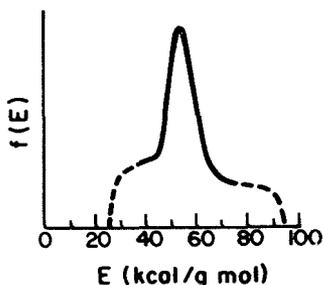
Fig. 6.1. Distribution of activation energies in Pitts' model (source: ref. 137).

interpretation would suggest that the part of the curve at low E corresponds to the formation of H_2O and CO_2 while the part at high E corresponds to the formation of hydrocarbon gases, CO and H_2. For example, reaction D2 which is the main methane forming step has activation energy about 70. The identification of the activation energies involved in the Pitt model with actual bond breaking energies provides the satisfaction that the model reflects some aspects of physical reality.

A further interesting implication of Pitt's model is manifested by attempting to match, in a least squares sense, Eq. (6.3) with the expression pertaining to a single first order reaction

$$W_v = W_v^* \left\{ 1-\exp \left[-t \, A \, \exp \, (-\overline{E}/RT) \right] \right\}$$ (6.4)

The two expressions would not agree very well over a broad range of temperatures, but in a limited range one can compute the value $\overline{E}$ that provides the best fit. The value of E calculated in this fashion turns out to be significantly lower than the mean of f(E). This behavior can explain to some degree the low activation energies determined in reference to the single reaction model.

Going back to Fig. 6.1 it is noted that curve f(E) has a single narrow peak, therefore, it could be well parametrized by two or three parameters, e.g. the location and width of the peak, without seriously compromising the ability to describe experimental weight loss data. Anthony et al. (refs. 126,136) utilized a Gaussian form,

$$f(E) = \frac{1}{(2\pi)^{\frac{1}{2}}\sigma} \exp \left[-\frac{1}{2\sigma^2} (E-E_0)^2 \right]$$ (6.5)

containing the two parameters E_0 and σ. They also treated W_v^* as an additional unknown parameter rather than identifying it with the proximate volatile matter. Thus, their model contained four parameters to be estimated from experimental data: W_v^*, A, E_0, σ, only one more than the primitive single first order reaction model. In the original papers of Anthony et al. (refs. 126,136), the limits of integration for Eq. (6.3) were taken $E_{min}=0$, $E_{max}=\infty$. In a later paper (ref. 125),

they used $E_{min}=0$ but treated E_{max} as an additional adjustable parameter. Table 6.1 lists the parameter values determined for two coals. For the lignite they determined two alternative sets which provided equally good agreement with the experimental weight loss data.

TABLE 6.1

Experimental parameter values for the model of Anthony et al.

Coal	Reference	W_v^* (%)	A (s^{-1})	E_o	E_{min} (kcal/gmole)	E_{max}	σ
Lignite	136	40.6	1.07×10^{10}	48.7	0	∞	9.38
"	"	40.6	1.67×10^{13}	56.3	0	∞	10.91
Bituminous	125	37.2	1.67×10^{13}	54.8	0	61.4	17.2

The model of Anthony et al. is sufficiently simple for combustion calculations provided some additional data are available regarding the heating value of the volatiles. An application to fluidized combustion was given in reference 138. In spite its practical success, this model might be criticized for its assumption of independent first order reactions. In later sections of this chapter, this assumption will be discussed in some detail.

6.1.3 Several first order reactions for individual products

In connection with the physical interpretation of the Pitt-Anthony model, it was pointed out that the range of activation energies could be divided into segments which can be tentatively associated with various classes of pyrolysis products. This idea leads quite naturally to describing individual product formation by independent first order reactions. A model of independent first order reactions, one for each product, was employed by the Bergbau-Forschung group (e.g. ref. 74). Suuberg et al. (refs. 64, 71, 72) used a more flexible approach by assuming that certain products can be formed by the breaking of two or more types of bonds, requiring a corresponding number of reactions. The number of reactions required for each product could be judged from the shape of the experimental yield-temperature curves. If each product precursor is recognized as an independent chemical species, its weight W_i changes according to

$$\frac{dW_i}{dt} = - A_i \exp (-E_i/RT) W_i \tag{6.6}$$

$$W_i(0) = W_i^*$$

Each product results from one to three reactions, corresponding to different

values of i and involving independent sets of parameters (W_i^*, A_i, E_i).

Suuberg et al. (refs. 64, 71, 72) conducted detailed measurements of pyrolysis products for a lignite and a high volatile bituminous coal using the captive sample technique (Chapter 3). In most experiments, the temperature-time history was a pulse consisting of a heating segment with rate about 1,000°C/s leading to the desired peak temperature. Immediately after the peak temperature was attained, the current was interrupted and the ensuing cooling segment with rate roughly - 200°C/s completed the pulse. Under these conditions, changing the peak temperature also changed the pulse width, i.e. the effective duration of the experiment. In some experiments, an isothermal temperature segment of 2-10 seconds followed the peak temperature to ensure complete devolatilization. The experiments employing protracted heating were used to determine W_i^*, while the experiments using the simple pulse were used to determine the kinetic parameters A_i, E_i.

Tables 6.2 and 6.3 list the parameter values determined for the lignite and the bituminous coal. Figures 6.2, 6.3 show measured and calculated yields for the lignite, corresponding to the parameters of Table 6.2, while Figures 6.4, 6.5 compare results for the bituminous coal, using the parameters of Table 6.3. The agreement between measurements and model calculations is very good for methane, ethylene and hydrogen (Figure 6.2) which evolve in a stepwise fashion with increasing peak temperature. The agreement is not as good for carbon oxides and water (Figure 6.3) where the experimental points seem to fall on a curve which is gradually increasing rather than stepwise. Within the conceptual framework of the model, the gradual evolution suggests a broad distribution of activation energies that cannot be accurately represented by one, two, or even three discrete values.

In the case of the bituminous coal (Figures 6.4, 6.5) the agreement between model curves and experimental results is good considering the inevitable scatter in the data. The tar yield in this case was calculated using the "evaporative diffusion model" combining kinetics and mass transfer (see Chapter 5). All other products were treated by pure kinetics.

In evaluating the independent reaction model, it should be kept in mind that the data exhibited in Figs. 6.2-6.5 involve total yields for given T-t pulses. No time-resolved data were available. The determination of the rate constants on the basis of cumulative yields becomes increasingly inaccurate with increasing temperature because of a "compensation effect" between the parameters A_i and E_i. In other words, different pairs describe the data equally well, provided a change in A_i is compensated by a commensurate change in E_i. This behavior explains the fact that a common A_i factor for all species other than H_2 and tar described satisfactorily the yields from the bituminous coal. It should also be noted

TABLE 6.2

Experimental parameter values for individual product formation in lignite pyrolysis (ref. 71).

Product	W_i^* (% of coal)	$\log (A_i/s^{-1})$	E_i (kcal/gmole)
CO_2	5.70	11.33	36.2
"	2.70	13.71	64.3
"	1.09	6.74	42.0
CO	1.77	12.26	44.4
"	5.35	12.42	59.5
"	2.26	9.77	58.4
CH_4	0.34	14.21	51.6
"	0.92	14.67	69.4
C_2H_4	0.15	20.25	74.8
"	0.41	12.85	60.4
HC^a	0.95	16.23	70.1
Tar	2.45	11.88	37.4
"	2.93	17.30	75.3
H_2O	16.50	13.90	51.4
H_2	0.50	18.20	88.8

a Hydrocarbons other than CH_4, C_2H_4 and tar

that several of the entries for log A in Table 6.2 are outside the range 12 to 16 pertaining to unimolecular decompositions. Likewise, the activation energy of 37.4 for the first tar forming reaction is much lower than the bond energies estimated in Chapter 3. This is not a serious criticism, however, in view of the great difficulty of multiple-parameter estimation from expressions containing sums of exponentials. The case of tar deserves special attention. The attempt to force the data into a single first order reaction results in a physically unacceptable set of parameters log A = 2.9, E = 13 kcal/mol, in line with the observation made in connection with the single reaction model. To improve on these numbers, the tar yields were fitted (ref. 71) by assuming a set of reactions with continuously distributed activation energies resulting in the parameter estimates log A = 15.4, E_0 = 68.9 kcal/gmole, σ = 11.4 kcal/gmole which

TABLE 6.3

Experimental parameter values for individual product formation in the pyrolysis of a high volatile bituminous coal (ref. 71).

Product	W_i^* (% of coal)	$\log (A_i/s^{-1})$	E_i (kcal/gmole)
CO_2	0.4	13	40
"	0.9	"	65
CO	0.4	"	55
"	2.1	"	65
CH_4	0.7	"	55
"	1.8	"	65
C_2H_4	0.2	"	55
"	0.6	"	65
C_2H_6	0.5	"	55
$C_3H_6+C_3H_8$	0.2	"	40
"	0.8	"	44
"	0.4	"	65
HC^a	0.4	"	55
"	0.8	"	65
HC^b	0.5	"	40
"	1.2	"	55
"	0.4	"	65
Tar	24.0	2.9	13
H_2O	5.4	13	35
H_2	1.0	17	90

a other hydrocarbon gases
b light hydrocarbon liquids

are much more in line with the rate parameters estimates of Chapter 3.

The models of Pitt, Anthony et al. and Suuberg et al. are very similar in their underlying assumptions. Both consider product evolution by parallel, independent and first order reactions operating on an initial amount W_i^* of
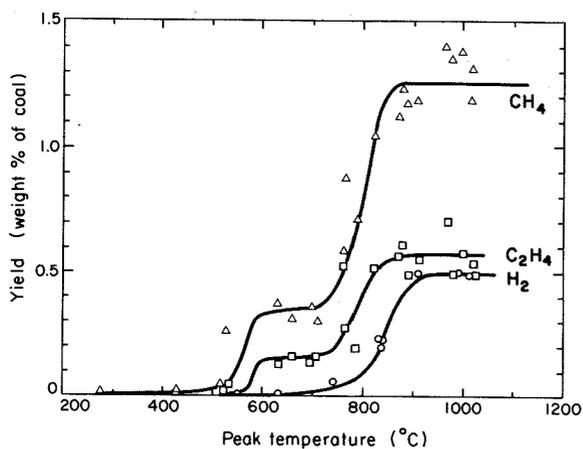
Fig. 6.2 Yields of CH_4, C_2H_4, H_2 from the pyrolysis of a lignite to different peak temperatures at 1 atm He and $1000^0C/s$ heating rate (source: refs. 63, 64).
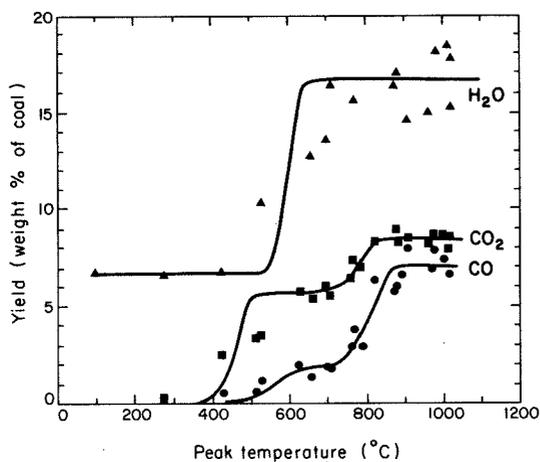

Fig. 6.3. Yields of H_2O, CO_2, CO from the pyrolysis of a lignite to different peak temperatures at 1 atm He and $1000^0C/s$ heating rate (source: refs. 63, 64).
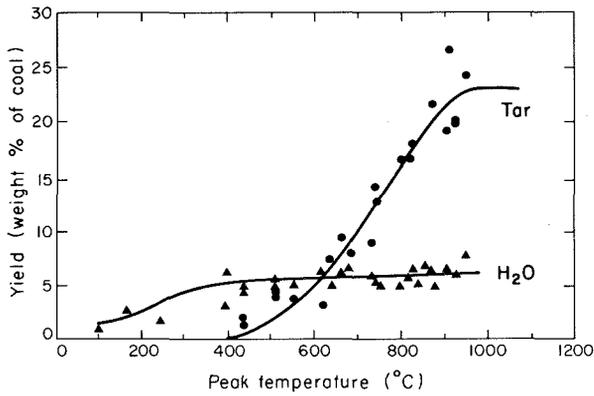
Fig. 6.4. Yields of tar and H_2O from the pyrolysis of a bituminous coal to different peak temperatures at 1 atm He and $1000^\circ C/s$ heating rate (source: refs. 63, 71).
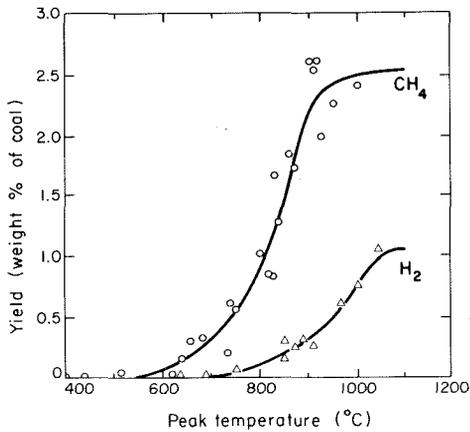

Fig. 6.5. Yields of CH_4, H_2 from the pyrolysis of a bituminous coal to different peak temperatures at 1 atm He and $1000^\circ C/s$ heating rate (source: refs. 63, 71).

volatile species precursors. When the reactions employed by Suuberg are assembled to describe the evolution of total volatiles, the collection of activation energies fall on a bell-shaped pattern, similar to the truncated Gaussian curve of Anthony et al.

The experimental studies of the Bergbau-Forschung group (ref. 74) employed a linearly increasing temperature-time history with rates varying from 10^{-2} °C/min (using an electric oven) to as high as 10^5 °C/min (using an electrical wire-mesh: the captive sample technique). The rates of production were measured continuously by mass spectroscopy providing unusually detailed kinetic information. Unfortunately, the production of tar could not be measured in this fashion. As an example of their results, we consider the production of ethane which they represented by a single reaction, with log A = 9.33, E = 42.7 kcal/mol, estimated from the kinetic curve corresponding to a heating rate of 2° C/min. The parameters for heating rates 10^4 °C/min were 9.95, E = 40.9. Although the model calculations matched the experimental curves quite well (see Fig. 6.6), the difference in the rate parameters (the rate constants differ by a factor of twelve at 600°C) requires examination. The discrepancy may be due to the inadequacy of a single reaction to describe the data or to the fact that the temperature-time history employed is not well suited for kinetic analysis. However, as can be seen from Figure 6.6 the ultimate yields represented by the areas below the curves do not differ by more than 15%, therefore, the data are not inconsistent with the basic premise of independent reactions.
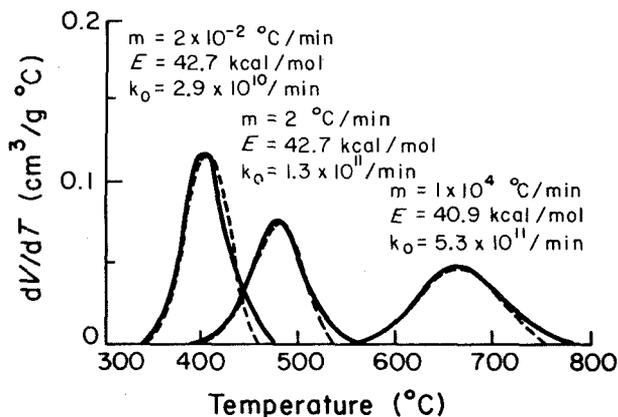

Fig. 6.6. Experimental (----) and calculated (——) rates of ethane production at different heating rates (source: ref. 74).

We have treated in considerable detail the models of independent first order reactions because of their attractive features, simplicity and successful

description of experimental product yields. One additional, and in our view important, attribute of these models is the generally reasonable values of the estimated parameters. With some exceptions, the activation energies are in the range of bond dissociation energies associated with functional groups encountered in coal (Chapters 2,3). The idea of product formation occuring by the breaking of specific bonds is straightforward and reasonable.

Undoubtedly, the network of pyrolysis reactions is much more complicated than a set of parallel and independent steps. The models to be discussed in the next section attempt to describe the coupling and competition between reactions leading to different products.

6.2   COMPETING REACTIONS

The consideration of competing reaction schemes has been prompted largely by data showing a negative correlation between the ultimate yields of tar and gases. Under some experimental conditions, an increase in the yield of gases is accompanied by a decrease in the yield of tar and vice-versa. The observed negative correlation could be due to the competition between purely chemical steps or to secondary reactions in conjunction with internal (intraparticle) or external (film) mass transfer limitations.

In chapter 4, we discussed pyrolysis product yields obtained by the captive sample or the entrained flow technique under conditions designed to minimize secondary reactions on the external surface of the particles or the hot surfaces of the equipment. Even under these conditions, however, external secondary reactions may adversely affect the yield of tar at high temperatures and long pyrolysis times. For example, the slight decline in the yield of tar above 800°C in Figures 4.4-4.7 is most likely due to such external secondary reactions. Anthony et al. (refs. 136,126) have pointed out that in most of the early experimental studies, low heating rates were invariably associated with densely packed coal particles, while high heating rates always required dispersed particles. Evidently, the dependence of tar and gas yields on heating rates observed in these studies cannot be attributed to the heating rate per se but rather to the larger or smaller external mass transfer limitations which are incidentally associated with the heating rate.

Intraparticle mass transfer hinders the removal of tar molecules and thereby increases the extent of secondary reactions in the interior of the particles. The extent of such internal secondary reactions increases with pressure and particle size as illustrated by the data presented in chapter 5. Clearly, to describe such mass transfer effects, it is necessary to consider secondary reactions in conjunction with the mass transfer process.

When the pressure is very low and the particles finely ground and well dispersed, the secondary reactions in the interior of the particle are largely

supressed. Under these conditions any competition between the yields of tar and gases would be due to purely chemical processes and would be governed by the only remaining operating variable, the temperature-time history. In the experimental work of the MIT group (refs. 63, 64, 71, 72) which devoted particular attention to eliminating secondary reactions, the temperature-time history was varied in three different ways. In the bulk of the experiments, the maximum temperature was varied at constant heating rate . The results of these experiments, which are generally similar to the results presented in Chapter 4, show yields of tar and gas to increase monotonically with temperature, and thus do not indicate the presence of competing reactions. The second type of temperature-time history employed consisted of fixing the maximum temperature while varying the heating rate in the range 250-10,000^{o}C/s (refs. 126, 63, 64, 71). For both the lignite and the high volatile bituminous coal that the experiments employed, the yields of tar and gases were within experimental error independent of the heating rate. The third variation of temperature-time history consisted of heating the coal sample to an intermediate temperature, cooling it and then subjecting it to a second and higher temperature pulse (refs. 63, 64, 71). Again, the yields depended on the maximum temperature and not on the details of the heating curve. However, this last type of operation was applied only to the lignite.

The experimental evidence leads to two major conclusions. If mass transfer limitations can be excluded, the product yields depend on the peak temperature and the length of time at that temperature rather on heating rate and other details of the temperature-time history. Future work may reveal some subtler dependencies but the data available to date can be well described by independent reaction models. To describe pressure and particle size effects, it is necessary to consider secondary reactions in conjunction with mass transfer processes. The description of combined mass transfer and kinetics is rather involved as discussed in the previous chapter.

The rest of this section reviews two coupled reaction models. The first model (ref. 129) specifically addressed to softening bituminous coals considers a series-parallel reaction scheme that can be naturally coupled with mass transfer processes. The second model does not include mass transfer limitations but ascribes the competitive evolution of tar and gases to purely chemical processes, namely a set of parallel reactions coupled by common reactants.

6.2.1 Model of Unger and Suuberg (ref. 129)

This model can be represented by the reaction scheme below. First of all, it is assumed that the fraction of coal consisting of the "inactive" macerals (fusinite, micrinite etc.) does not participate in the pyrolysis. The remaining fraction, consisting of the vitrinite, exinite and resinite macerals reacts in the

manner indicated below. Water and carbon dioxide evolve by first order reactions (constants k_{i1}, k_{i2}) independent of other subsequent steps. In parallel, coal is converted to an intermediate material called "metaplast," by a first order reaction with constant k_m. The term metaplast was introduced in an early model by Chemin and van Krevelen (ref. 139). The conversion to metaplast proceeds by dissociation of bridges between structural units, therefore, the metaplast molecules, structurally similar to coal, have a distribution of molecular weights. This distribution is assumed to be normal and its mean and standard deviation are treated as adjustable parameters remaining constant during pyrolysis.
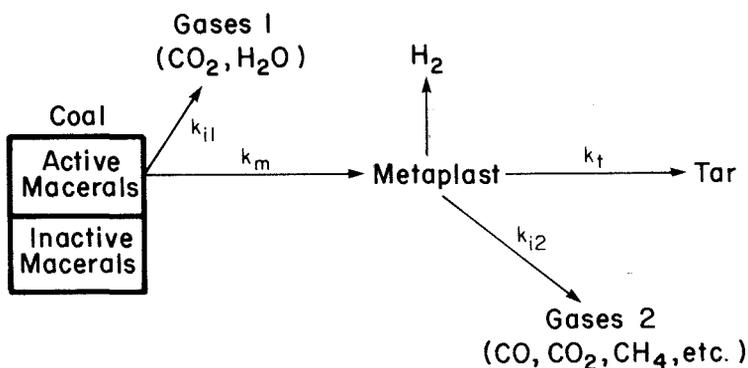
Once formed, metaplast participates in further reactions. The first is polymerization to larger molecules, accompanied by evolution of hydrogen. The effect of this polymerization on the mean and standard deviation of the molecular weight distribution is not taken into account. The metaplast also forms a variety of light products: CO_2, CH_4, C_2H_4, C_2H_6, C_3H_6, C_3H_8, higher hydrocarbon gases and hydrocarbon liquids by parallel, independent reactions with constants k_{i2}. These reactions consume hydrogen to saturate the precursor radicals, hence, their rate is taken to be proportional to the instantaneous content of aliphatic hydrogen in the metaplast.

The final step is the conversion of metaplast to tar. Tar consists of vapors of metaplast fragments, therefore, this step represents the transfer of tar molecules from the condensed phase (metaplast) to the gas phase outside the coal particle. The rate of this mass transfer step is calculated by solving the diffusion problem in the stagnant region surrounding the particle and turns out to be proportional to the vapor pressure of metaplast molecules. The mass transfer problem was discussed in some detail in the previous chapter.

Reference 129 does not include mathematical derivations but gives the parameter values used in the calculations and the comparisons with experimental data. While this model contains a larger number of adjustable parameters, compared to the independent reaction models, it provides a more fundamental description of the pyrolysis chemistry. By virtue of including secondary reactions it allows the description of pressure and particle size effects. The model is a promising one although it requires further work relative to the formation and repolymerization of metaplast and to possible intraparticle mass transfer limitations.

6.2.2   Model of Solomon (refs. 61, 78)

This model describes purely chemical processes and utilizes the following assumptions:

(i)   At any instant during pyrolysis, coal is composed of two materials, tar-forming and non-tar-forming, with weights W_T, $W-W_T$, where initially $W=W_o$, $W_T=W_{oT}$. This constitutes the vertical division in Figure 6.7.

(ii)   The tar-forming and the non-tar-forming materials are in turn composed of nonvolatile carbon and certain constituents that are precursors to volatile products e.g. H_2O, heavy hydrocarbons, light hydrocarbons, etc. These correspond to the horizontal division in Figure 6.7. The mass fractions of these constituents are the same in the tar-forming and non-tar-forming materials and are denoted by Y_i with initial values Y_{oi}.

(iii) Pyrolysis consists of two types of reactions denoted by DT and DG_i. Reaction DT generates tar molecules by splitting off *vertical* slices containing the instantaneous or current composition of the material. Reactions DG_i produce volatile products by splitting off *horizontal* slices of precursors across both the tar-forming and the non-tar-forming material. Solomon has aptly made the analogy with a bowl of soup being consumed by removing spoonfuls (DT) and by evaporation of ingredients (DG_i).

(iv)   The reactions DG_i have the same rates in the tar-forming and non-tar-forming materials, therefore, the mass fractions Y_i remain equal in the two materials. Since Y_i change with time, the composition of evolving tar molecules also varies with time although it continues being identical to the composition in the remaining coal.

(v)   The reactions DT and DG_i are all independent and obey first order kinetics. Because the definitions and notation in refs. 61, 78 are somewhat difficult to follow, the derivations given below employ a different notation. The instantaneous weights of the various constituents in the coal undergoing pyrolysis will be denoted by W_i. In particular W_{nvc} will denote the weight of the horizontal slice representing the nonvolatile carbon. This term is somewhat of a misnomer
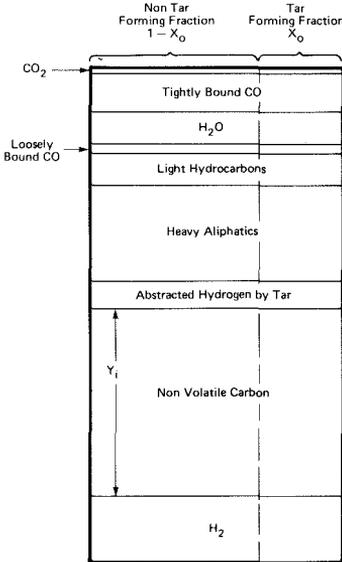
Fig. 6.7. Precursors of various pyrolysis products
according to Solomon's model (source: ref. 61).

because although nonvolatile carbon is not affected by any of reactions DG, it is removed as part of the departing tar molecules. The quantity Y_{nvc} $(W-W_T)$ which represents the weight of nonvolatile carbon in the non-tar-forming material is constant,

$$W_{nvc}(W-W_T) = Y_{o,nvc} (W_o-W_{oT}) \tag{6.7}$$

and proportional to the number of "moles" in that fraction. Likewise, Y_{nvc} $\cdot W_T$ is proportional to the number of "moles" in the tar-forming material. Assumption (v) implies

$$\frac{d}{dt} \left(W_T Y_{nvc} \right) = - k_T W_T Y_{nvc}$$

which under isothermal conditions is integrated to

$$W_T Y_{nvc} = Y_{oT} Y_{o,nvc} \exp (-k_T t) \tag{6.8}$$

The composition variable

$$y_i = \frac{Y_i}{Y_{nvc}} = \frac{Y_i(W-W_T)}{Y_{nvc}(W-W_T)}$$

is proportional to the "mole fraction" of constituent i in the non-tar-forming material and in the coal as a whole, since the composition of both materials is the same. Assumption (v) then implies that under isothermal conditions

$$\frac{dy_i}{dt} = - k_i y_i$$

therefore,

$$\frac{Y_i}{Y_{nvc}} = \frac{Y_{oi}}{Y_{o,nvc}} \exp(-k_i t) \qquad (6.9)$$

Relations (6.7)-(6.9) allow the computation of all quantities of interest. Adding (6.7) and (6.9) yields

$$Y_{nvc} W = Y_{o,nvc}(W_o-W_{oT}) + W_{oT} Y_{o,nvc} \exp(-k_T t) \qquad (6.10)$$

therefore, from (6.9)

$$W_i = Y_{oi}(W_o-W_{oT}) \exp(-k_i t) + Y_{oi} W_{oT} \exp[-(k_i+k_T)t] \qquad (6.11)$$

The total weight is obtained by summing over i,

$$W = (W_o-W_{oT}) \sum_i Y_{oi} \exp(-k_i t) + W_{oT} \sum_i Y_{oi} \exp[-(k_i+k_T)t] \qquad (6.12)$$

where $k_i=0$ for i=nvc. The composition in the char (remaining coal), $Y_i=W_i/W$ can be calculated from (6.11) and (6.12).

The instantaneous production of constituent i as a gas (and not with tar) is given by $k_i W_i$, hence using (6.11) we find the cumulative production of gas i as

$$\int_o^t k_i W_i dt = Y_{oi}(W_o-W_{oT}) [1-\exp(-k_i t)]$$

$$+ Y_{oi} W_{oT} \frac{k_i}{k_i+k_T} \left\{ 1-\exp[(k_i+k_T)t] \right\} \qquad (6.13)$$

The ultimate production of gas i (t → ∞) is

$$Y_{oi}(W_o-W_{oT}) + Y_{oi} W_{oT} \frac{k_i}{k_i+k_T} \qquad (6.14)$$

Summing over all i≠nvc we find the ultimate weight of gases produced as

$$(1-Y_{o,nvc})(W_o-W_{oT}) + W_{oT} \sum_i \frac{Y_i k_i}{k_i+k_T} \qquad (6.15)$$

The ultimate weight of char is obtained from (6.12) as

$$W_\infty = Y_{o,nvc} \, (W_o - W_{oT}) \tag{6.16}$$

The ultimate weight of tar produced is the difference between $(W_o - W)$ and the weight of gases produced. Using (6.15) and (6.16) the weight of tar is obtained as

$$W_{oT} - W_{oT} \sum_i \frac{Y_{oi} k_i}{k_i + k_T} \tag{6.17}$$

According to the above expressions the ultimate weight loss is independent of temperature but the ratio of gases to tar varies with temperature due to the relative activation energies of k_i and k_T. Since the activation energies of k_i are generally larger than that of k_T, the ultimate yield of gases generally increases with temperature at the cost of the yield of tar.

The various stoichiometric (X_o, Y_{oi}) and kinetic (k_i, k_T) parameters of the model were estimated by comparisons with experimental data and the estimated values are given in ref. 61. Although the procedure used in the estimation was not explained in detail, it probably involved some trial and error in as much as expressions (6.14) giving the yield of gaseous products include stoichiometric as well as kinetic parameters. The agreement between model predictions and experimental data may be judged from Figures 4.4 - 4.11 where the solid lines represent model calculations. The agreement is good in most cases, however, because of the scatter in the data, the comparisons do not provide a critical test concerning competitive product evolution and other assumptions in this model.

In comparing the models of Solomon (ref. 61) and Suuberg et al. (refs. 64, 71, 72) we note that both employ essentially the same number of adjustable parameters. Although Solomon's model appears more flexible allowing for the competitive evolution of gases and tar, its ability to represent experimental data does not appear to be superior to that of the independent reaction model. The distinction between the two classes of reactions DT and DG_i is useful from the theoretical standpoint, however, the a priori division between tar-forming and non-tar-forming materials of identical composition is clearly empirical. The estimated model parameters include very low activation energies for reaction DT and several of the DG_i reactions. This may again arise from representing several reactions of different activation energies by a single reaction.

6.3 DETAILED CHEMICAL MODELS

In principle, a detailed chemical model should describe pyrolysis in terms of coal's functional groups and their elementary reactions. Chapters 2 and 3 gave a survey of structural and kinetic information that might be useful for this purpose. However, detailed chemical modeling remains hampered by many serious difficulties. Available structural information continues being tentative and qualitative. For example, the relative concentrations of methylene, ethylene and

ether bridges, constituting one of the most important structural features, have not
yet been quantified. A second difficulty is the large number of individual ele-
mentary reactions making the mathematical analysis very unwieldy. A third yet
difficulty is the lack of reliable physical properties needed for characterizing
mass transfer within the pyrolyzing particles. In view of these difficulties the
efforts to develop a reliable model based on functional groups and chemical reac-
tions have made very limited progress. In the first section of this chapter we
outline a recent kinetic model by Gavalas, Cheong and Jain (refs. 65, 133, 134)
and in the second section we discuss possible directions for future kinetic modeling

6.3.1 A detailed kinetic model (refs. 65, 133, 134)

This chemical model rests on the following general assumptions:
(i) Coals belonging to a broad range of rank, e.g. subbituminous or bituminous,
can be characterized by a common set of functional groups, with different coals
differing by the concentrations of these functional groups.
(ii) At high temperatures the functional groups react by well known free radi-
cal mechanisms.

Since most functional groups are substituents to aromatic nuclei their
reactivity depends on the type of nucleus and the existence of other neighbor-
ing substituents. For example, the two bond dissociation reactions
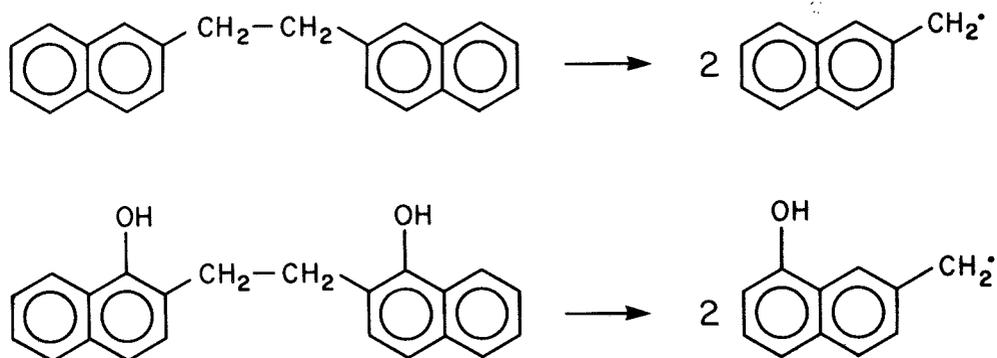
involve the same group, the ethylene bridge. The second reaction, however, is
much faster than the first on account of the presence in the ortho position of
the activating hydroxyl group. A complete description of the kinetics must dis-
tinguish between those ethylene bridges that are associated with hydroxyl groups
in the ortho position and those that are not. A description at this level of
detail would require consideration of a very large number of chemical structures
and would be completely out of line with experimental information. To simplify
the situation, the following additional assumption is made:

(iii) Any given functional group is exposed to an average environment of other groups, therefore, its reactivity depends only on the *concentration* of other groups.

Assumption (iii) is subject to certain exceptions that can be illustrated by the following example:

$$\phi-CH_2-CH_2-\phi' \rightarrow \phi-CH_2\cdot + \phi'-CH_2\cdot \qquad (a)$$

$$\phi-\overset{\cdot}{C}H-CH_2-\phi' \rightarrow \text{no dissociation} \qquad (b)$$

The dissociation of the ethylene group is completely suppressed in the presence of another group, the α radical. In this case it is necessary to calculate the fraction of ethylene bridges that *do not carry* an α radical. Similar restrictions apply in the presence of double bonds. Such restrictions, or constraints, are taken into account by calculating the configurations of functional groups that are susceptible to reactions. The concentration of these *reactive configurations* is calculated using another yet simplifying assumption:

(iv) At any instant, the functional groups are located completely randomly, subject to some obvious constraints (e.g. no two radicals or radical and double bond can coexist on a single carbon atom). To calculate the concentration of reactive configurations in terms of the concentrations of functional groups requires the solution of a combinatorial placement problem which is solved by standard techniques akin to those used in statistical mechanics.

Once the concentration of reactive configurations has been calculated, the rate of generation of all volatile products other than tar can be calculated. To calculate the rate of tar production, certain additional constraints must be considered. Tar molecules contain, by definition, one or more structural units (see chapter 2), therefore, one or more aromatic nuclei. The vapor pressure and diffusion coefficients of these molecules in the condensed phase decrease rapidly with increasing molecular weight. Thus tar precursor molecules (metaplast) generated in the condensed phase have very small probability of evolving to the gas phase unless they contain only one structural unit.

Having placed a molecular size constraint, we note that the rate of generation of tar molecules is the product of three factors. The first is the concentration of precursor units *connected by a single bridge* to the coal phase. The concentration of precursor units is calculated by a combinatorial placement technique similar to the one employed for reactive configurations. The second is the dissociation rate of the bridges. The third factor is the probability that a unit that has become free by bridge dissociation will be transferred to the gas phase, rather than participate in further reactions in the coal phase.

The last factor is quite complicated as it involves mass transfer processes in the condensed phase and the pore space. Considering first the condensed phase, a free unit produced by a dissociation reaction such as

$$\phi-CH_2-CH_2-\phi\acute{} \rightarrow \phi-CH_2\cdot + \phi\acute{}-CH_2\cdot$$
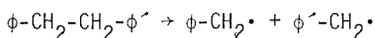
is subject to immediate recombination by the reverse reaction (cage effect) unless it can quickly transfer to the pore space. Likewise, a free unit formed by

$$H\cdot + \phi-CH_2-\phi\acute{} \rightarrow \phi-CH_2\cdot + \phi\acute{}H$$
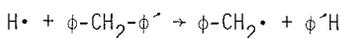
must diffuse to the surface of a pore or a bubble before escaping to the gas phase. During this diffusion process, the unit is subject to recombination with free radical sites on the coal matrix. Because these phenomena are very difficult to quantify, the model introduces an empirical adjustable parameter X describing the probability that a free unit formed by dissociation reactions (metaplast molecule) will be transferred to the gas phase rather than recombine in the coal phase. In some computer calculations X was given values in the range 0.1-0.2. Once in the pore phase, a free unit was assumed to transfer outside the particle with no further diffusional limitations. This very crude way of handling intraparticle mass transfer fails to account for the effects of pressure and particle size discussed in chapter 5.

Having defined the main physicochemical assumptions we can summarize the model by the block diagram of Fig. 6.8. Blocks 1,2 define the functional groups whose concentrations characterize the state of the coal at any instant during pyrolysis. Some sample calculations discussed in ref. 102 employed fifteen functional groups including two radicals, alpha and beta. Block 3 includes the calculations of the concentrations of reactive configurations referred to previously. The information about reaction mechanisms and rate parameters is introduced through block 4 which in combination with block 3 derives expressions for the rates of individual reactions (block 5). Block 6 includes the calculations of the rate of tar production. The rate of change of any given functional group consists of a direct term, due to one or more elementary reactions, and an indirect term due to the loss of tar molecules carrying the functional group under question. These two terms are combined in the differential equations describing the evolution of the state variables (block 7).

Figure 6.9 is a sample of model calculations compared with a few experimental points for a high volatile bituminous coal. The kinetic parameters used in the calculations were specified as follows. The initial concentrations of functional groups were estimated from elemental analysis and nmr data of pyrolysis tars. Most kinetic parameters were taken from the literature or estimated by thermochemical kinetics while a few parameters were adjusted to get reasonable agreement with experimental data. The adjusted values were in all cases within physically reasonable limits.

Using this set of parameters as a base case, sensitivity calculations were carried out varying one parameter at a time and recomputing the product yields.
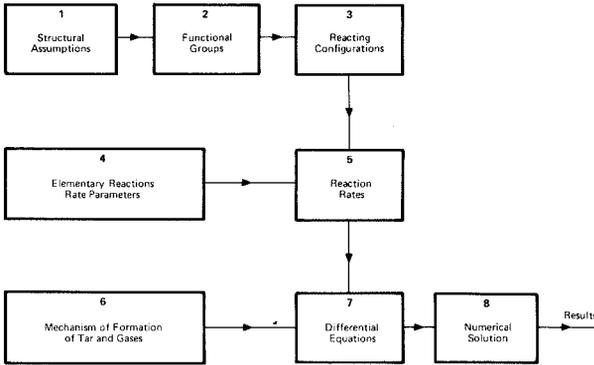
```
┌─────────────┐   ┌─────────────┐   ┌─────────────┐
│      1      │   │      2      │   │      3      │
│ Structural  │──▶│ Functional  │──▶│  Reacting   │
│ Assumptions │   │   Groups    │   │Configurations│
└─────────────┘   └─────────────┘   └─────────────┘
                                           │
                                           ▼
┌─────────────┐                    ┌─────────────┐
│      4      │                    │      5      │
│Elementary Reactions│────────────▶│  Reaction   │
│Rate Parameters│                  │    Rates    │
└─────────────┘                    └─────────────┘
                                           │
                                           ▼
┌─────────────┐   ┌─────────────┐   ┌─────────────┐   Results
│      6      │   │      7      │   │      8      │
│Mechanism of Formation│────────▶│Differential│──▶│ Numerical │──▶
│of Tar and Gases│     │Equations │   │ Solution  │
└─────────────┘   └─────────────┘   └─────────────┘
```

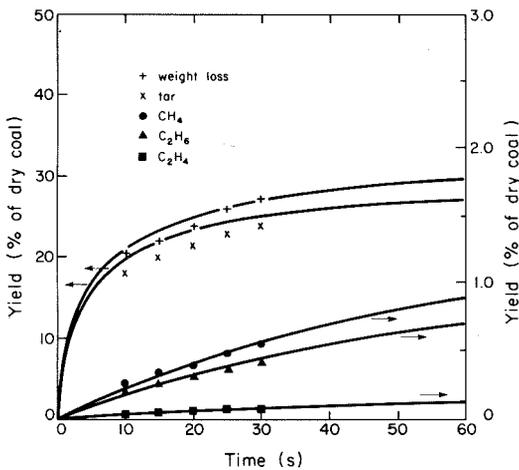Fig. 6.8. Organization of the model of Gavalas et al.
(refs. 133, 134).

Fig. 6.9. Calculated (———) and experimental product yields
from the pyrolysis of a hvc bituminous coal, "Kentucky No. 9,"
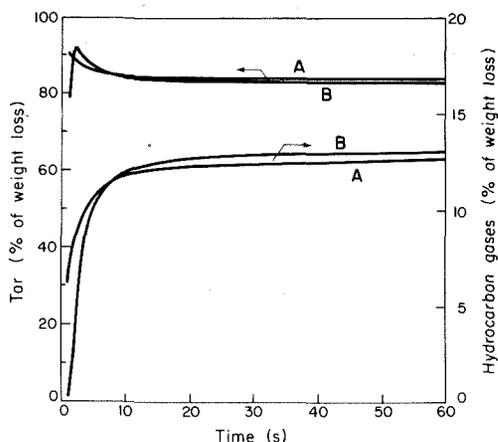at 510°C and 1 atm He (source: ref. 134).

Fig. 6.10. Calculated effect of temperature-time history on relative product yields from the pyrolysis of an hvc bituminous coal, "Kentucky No. 9," at 1 atm He. A: isothermal at 600°C; B: 400°C to 600°C linear in 2s followed by isothermal at 600° (source: ref. 65).

The parameter with the greatest effect on the results was the rate constant for bridge dissociation (reaction D5, Ch3). Other important parameters were the average number of bridges per structural unit (extent of cross linking) and the rate constants for radical dissociation reactions (DB1-DB4, chapter 3).

To test the effect of temperature-time history, calculations were performed for two different conditions. One was isothermal pyrolysis at 600°C. The other consisted of a period of two seconds of linearly rising temperature, from 400 to 600°C, followed by isothermal operation at 600°C. The isothermal operation resulted in a slightly higher weight loss (about 2.5%), slightly higher yield of tar and slightly lower yield of gases. Figure 6.10 compares relative product yields under the two temperature-time histories. The difference in the relative yields is slight, especially for tar. Before drawing more general conclusions, calculations should be made for several other types of temperature-time histories.

In view of the use of several adjustable parameters, the comparison between calculated results and the few experimental points (Fig. 6.9) have very little significance, other than indicating the plausibility of the reaction scheme and pointing out the main pathways for the production of various products. As formulated in refs. 133, 134 the model suffers from two serious defects. One

is the complexity of the rate expressions resulting from the combinatorial
calculation of reactive configurations. The other is the failure to simplify
the reaction network by eliminating a number of relatively unimportant functional
groups and reactions. The possibilities for such simplifications have emerged
from recent structural and model compound studies but have yet to be exploited
in kinetic modeling. The next subsection will thus be limited to a qualitative
discussion of these possibilities.

6.3.2 Further ideas on kinetic modeling

Recent structural and kinetic studies on whole coal, coal-derived liquids and
coal-like model compounds have provided a sharper focus on the functional groups
and chemical reactions most significant in pyrolysis. This newer information
suggests a revision and simplification of the list of functional groups and reac-
tions employed in refs. 133, 134. By restricting the number of functional groups,
it is no longer essential to utilize random distributions, hence, the rate expres-
sions can be considerably simplified. At the same time the hydroaromatic struc-
tures attain a more crucial status in the overall reaction network. The following
is a revised list of functional groups and chemical reactions that might be suit-
able for future modeling efforts.

functional groups

To attain a manageable model it is essential to keep the number of functional
groups at a minimum. It is thus almost necessary to consider an average aromatic
nucleus, common to all structural units. The average nucleus would contain a cer-
tain number of aromatic carbons and hydrogens and heteroaromatic oxygen sulfur
and nitrogen. These numbers are not integers because they represent not any par-
ticular ring system, but an average ring system.

The substituents on the aromatic nucleus may be limited to methyl and phenolic
hydroxyl. The exclusion of aliphatic chains longer than methyl is suggested by
the work of Deno and coworkers (refs. 12-14) but may be inappropriate for certain
coals.

Hydroaromatic structures are very important and must be carefully considered.
The four groups below have been tentatively suggested in recent structural
studies.

| 1 | 2 | 3 | 4 |
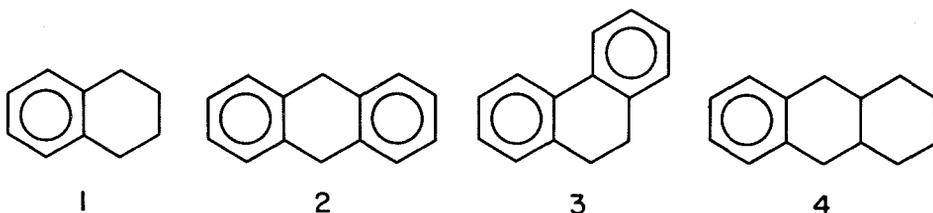
These groups have not been directly identified but have been inferred from the interpretation of various analytical data. The selective oxidation studies of Deno and coworkers suggest the absence of unsubstituted tetralin structures, although they allow for the possibility of methyl-substituted tetralin structures (ref. 12). Likewise, structure 2 was suggested as predominant in an Illinois No. 6 coal, while structure 3 was only indicated as possible. Structure 4 has been employed in order to explain the relatively low ratio of aliphatic hydrogen to aliphatic carbon determined from 'H and ^{13}C nmr spectra of coal extracts (ref. 140). Other complex multiring structures can also be employed for this purpose Some recent unpublished functional group analysis of coal derived liquids by this author also strongly suggests the presence of complex hydroaromatic structures like 4.

The final type of groups are the bridges. Most recent publications suggest methylene ($-CH_2-$) and diaryl ether ($-O-$) as the most abundant bridges between aromatic nuclei. In this respect it must be noted that structure 2 above can be considered either as a hydroaromatic structure or as two methylene bridges. However, in the process of pyrolysis it is unlikely that both bridges could be dissociated before other reactions take place. Along the same line of thought, the biphenyl bond is not meaningfully considered as a bridge because it does not dissociate by thermal means. Finally, ethylene bridges $-CH_2-CH_2-$ have not been specifically identified or excluded on the basis of analytical data.

chemical reactions

The volume of evidence favors free radical rather than pericyclic (concerted) mechanisms, although the latter may play some limited role. One reaction that probably occurs by a non-radical mechanism is the condensation of phenolic groups.
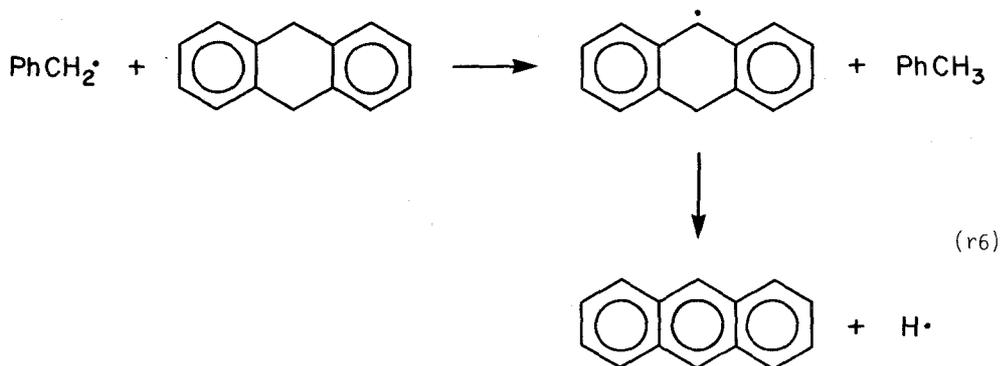
Limiting attention to free radical mechanisms we first consider the set of propagation reactions which determine the relative yield of various products. Prominent among these are the reactions of hydrogen atoms and methyl radicals. The hydrogen atoms participate in two types of reactions, hydrogen abstraction and addition illustrated by the examples

$$H\cdot + PhCH_3 \rightarrow H_2 + PhCH_2\cdot \tag{r1}$$

$$H\cdot + PhCH_3 \rightarrow PhH + CH_3\cdot \tag{r2}$$

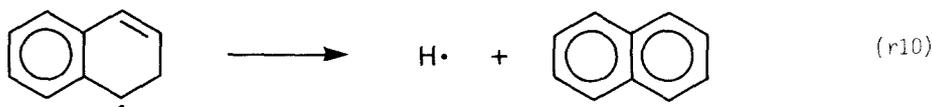$$H\cdot + PhCH_2Ph \rightarrow PhCH_2\cdot + Ph'H \tag{r3}$$
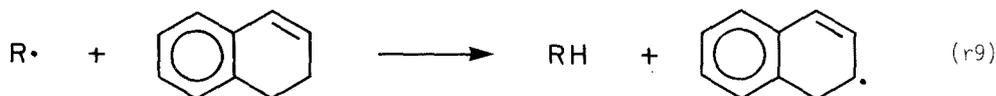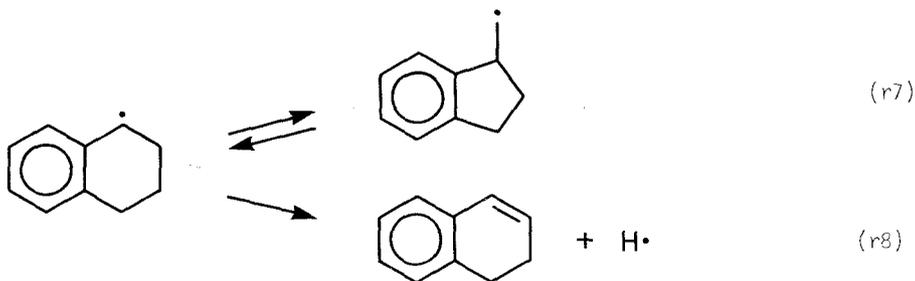
Reactions (r2) and (r3) have already been discussed in section 3.6. They are important steps for bridge dissociation (r3) and methane formation (r2). Methyl radicals react quite similarly, e.g.
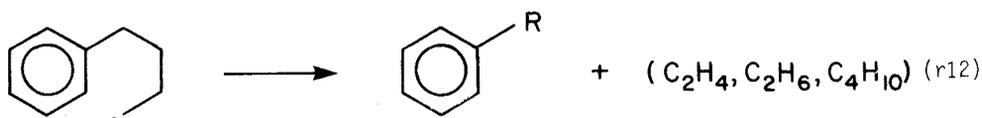
$$CH_3\cdot + PhCH_3 \rightarrow CH_4 + PhCH_2\cdot \tag{r4}$$

$$CH_3\cdot + PhCH_2Ph \rightarrow PhCH_2\cdot + Ph'CH_3 \tag{r5}$$

Alpha radicals participate in hydrogen exchange reactions such as

$$PhCH_2^{\bullet} \; + \; \text{[anthracene-like structure]} \longrightarrow \text{[radical structure]} \; + \; PhCH_3$$

$$\downarrow \qquad\qquad\qquad (r6)$$

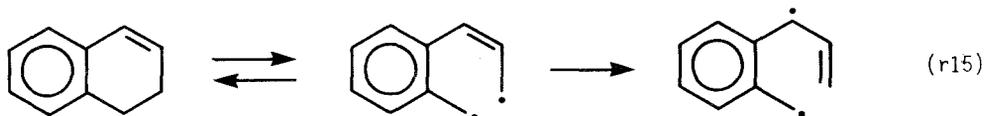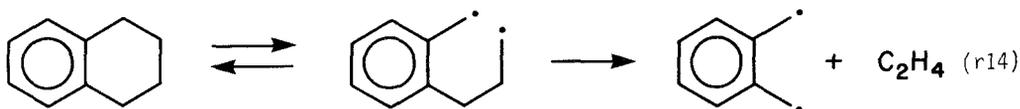$$\text{[anthracene structure]} \; + \; H^{\bullet}$$

Reaction (r6) serves to saturate alpha radicals and at the same time regenerates hydrogen atoms. While the hydroaromatic groups 2,3 react fairly simply as in (r6) above, the groups 1,4 react in a more complicated way. The propagation reactions of group 1 (tetralin-like structure) are summarized below, where the phenyl ring could actually be a naphthyl or other ring system. Reaction (r7) leads to methylindan while (r8) leads to the relatively unstable dihydro-naphthalene which eventually ends up as naphthalene (r10). The addition reaction (r_{11}) can be followed by various hydrogen abstractions and dissociations

$$\text{[tetralin radical]} \rightleftharpoons \text{[methylindan radical]} \qquad (r7)$$

$$\searrow \text{[dihydronaphthalene]} \; + \; H^{\bullet} \qquad (r8)$$

$$R^{\bullet} \; + \; \text{[dihydronaphthalene]} \longrightarrow RH \; + \; \text{[dihydronaphthalenyl radical]} \qquad (r9)$$

$$\text{[dihydronaphthalenyl radical]} \longrightarrow H^{\bullet} \; + \; \text{[naphthalene]} \qquad (r10)$$

$$H\cdot \ + \quad \text{(naphthalene/tetralin)} \longrightarrow \quad \text{(dihydronaphthalene radical)} \qquad (r11)$$
$$(\text{or } CH_3\cdot)$$

$$\text{(radical)} \longrightarrow \text{(Ph-R)} \ + \ (C_2H_4, C_2H_6, C_4H_{10}) \qquad (r12)$$

resulting in C_2-C_4 hydrocarbons. The point to be emphasized here is that light hydrocarbon gases other than methane need not arise from aliphatic chains but may largely arise from the decomposition of hydromatic structures as illustrated by reactions (r11), (r12).

Among various possible initiation reactions, only three are relatively energetically favorable,

$$Ph-CH_2-CH_2-Ph' \rightleftarrows Ph-CH_2\cdot \ + \ Ph'-CH_2\cdot \qquad (r13)$$

$$\text{(structure)} \rightleftarrows \text{(biradical)} \longrightarrow \text{(structure)} \ + \ C_2H_4 \qquad (r14)$$

$$\text{(structure)} \rightleftarrows \text{(biradical)} \longrightarrow \text{(structure)} \qquad (r15)$$

where the phenyl ring could be any aromatic ring system. Which of reactions (r13-r15) is more important is not known at this time because of uncertainties about the concentration of ethylene bridges and the magnitude of the cage effect on the rate of (r13). The kinetics of reactions (r14), (r15) are also poorly understood as they involve ring opening with formation of biradicals. As a result of these uncertaintaies the rate of initiation reactions cannot at this point be predicted from first principles, even if complete structural information was available.

Termination reactions are due almost entirely to recombination of the relatively abundant alpha radicals. The rate of this recombination is controlled by diffusion and might be negligible during the period of rapid product formation.